

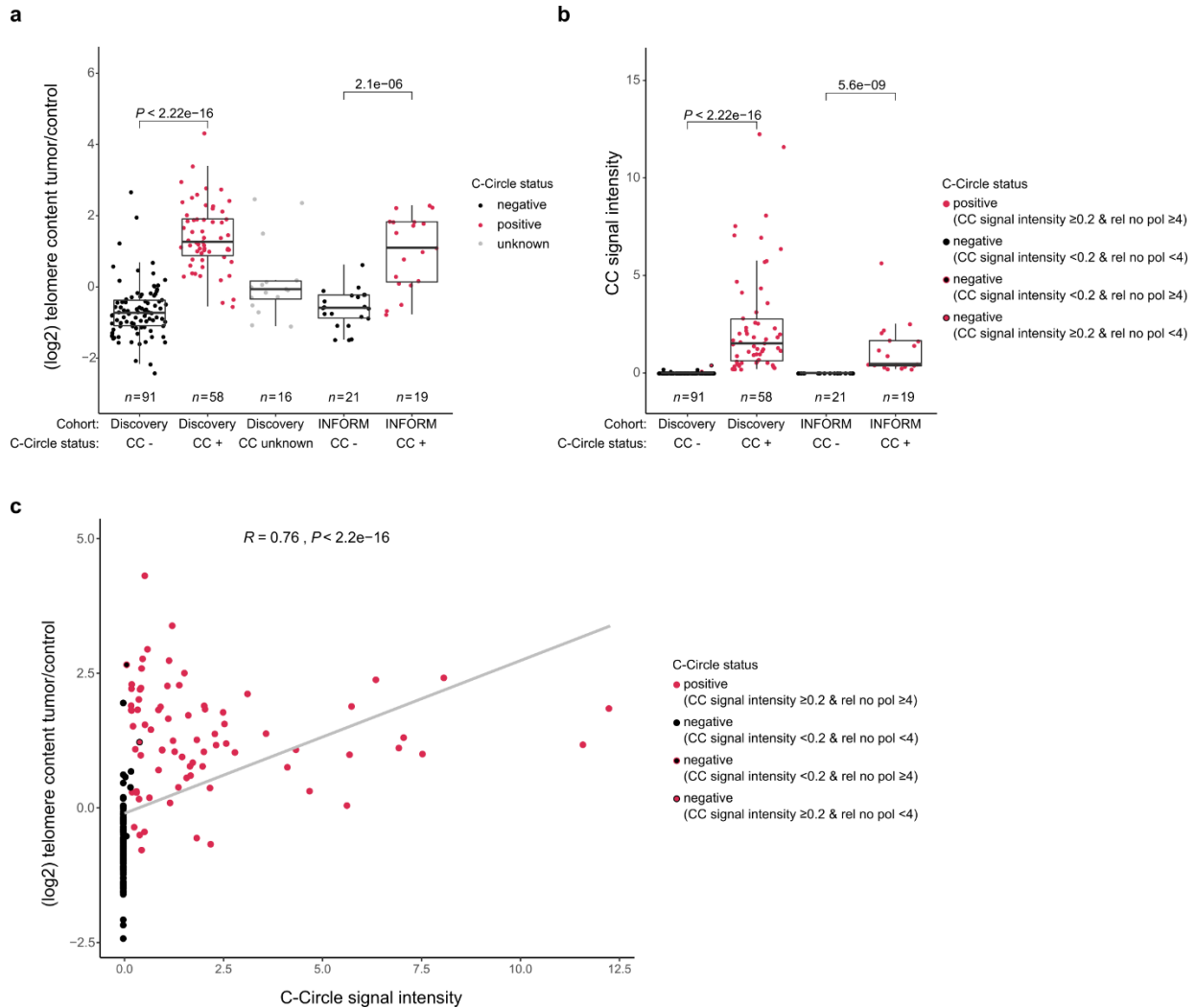
## Supplementary Information:

### Alternative lengthening of telomeres in childhood neuroblastoma from genome to proteome

*Hartlieb and Sieverling et al.*

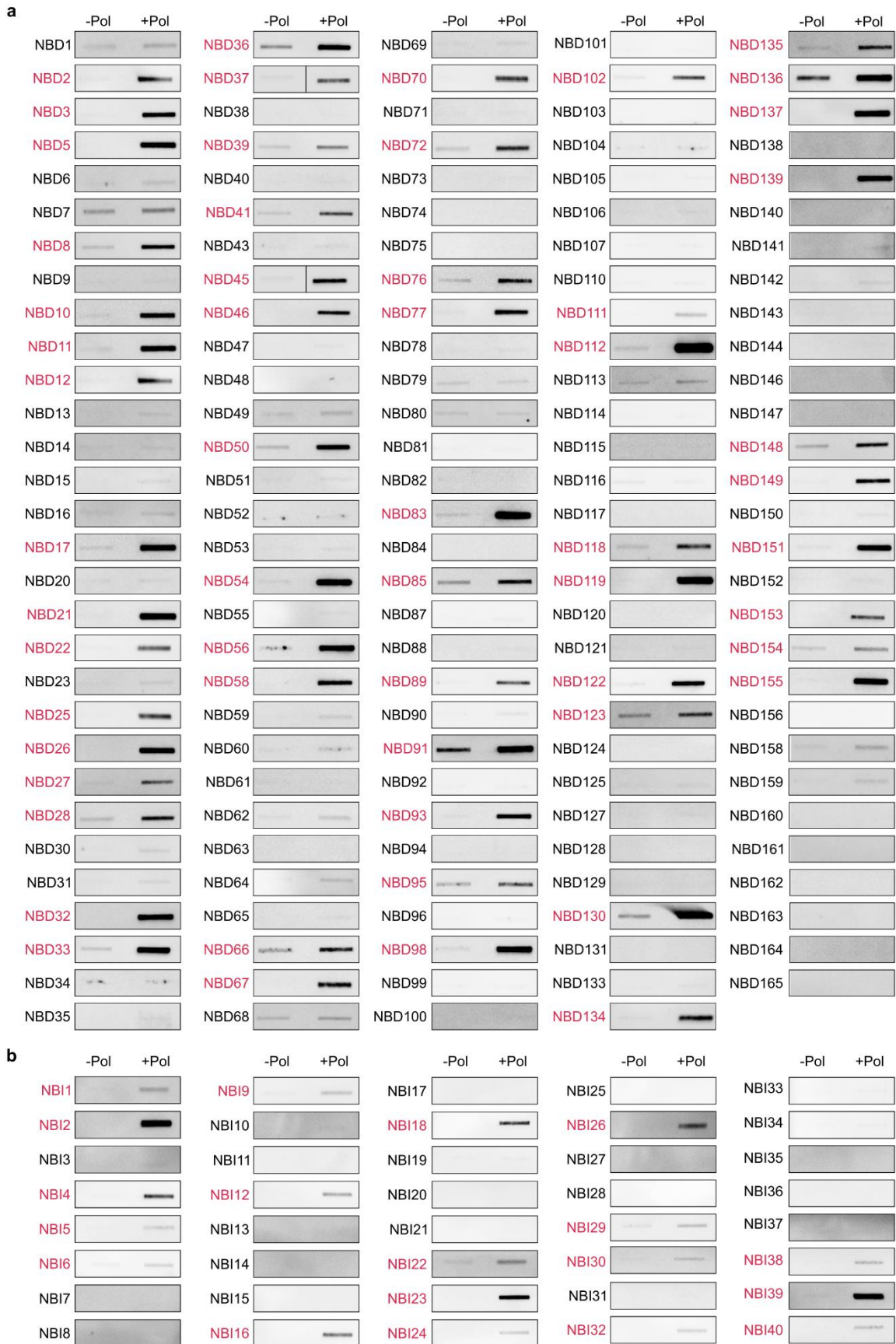
I. Supplementary Figures.....	- 2 -
Supplementary Figure 1: Telomere content and C-Circle intensity of discovery and INFORM cohort	- 2 -
Supplementary Figure 2: C-Circle status of discovery and INFORM cohort .....	- 4 -
Supplementary Figure 3: Silencing of <i>TERT</i> locus, telomerase activity and raw TERRA counts .....	- 6 -
Supplementary Figure 4: Comparison of matching primary and relapse pairs.....	- 7 -
Supplementary Figure 5: Combined <i>MYCN</i> and telomere FISH.....	- 8 -
Supplementary Figure 6: Most frequent differentially mutated genes in ALT-positive tumors.....	- 10 -
Supplementary Figure 7: <i>CDK4/CCND1</i> expression and mutations in Telnet genes.....	- 12 -
Supplementary Figure 8: Overall copy number patterns of ALT-positive tumors compared to ALT negative tumors of the discovery cohort. ....	- 13 -
Supplementary Figure 9: <i>SYNE1</i> and <i>PTPRD</i> .....	- 15 -
Supplementary Figure 10: Mutational landscape of INFORM cohort.....	- 16 -
Supplementary Figure 11: Comparison of mRNA and protein data .....	- 17 -
Supplementary Figure 12: Exon specific expression of <i>ATRX</i> and most frequent mutations in ALT-positive <i>ATRX</i> wild-type neuroblastomas.....	- 20 -
Supplementary Figure 13: Mutations in <i>ATRX/DAXX</i> interaction partners.....	- 22 -
Supplementary Figure 14: Chromatin state at <i>SatII</i> and <i>SatIII</i> sequences.....	- 23 -
Supplementary Figure 15: Features of telomeric repeat loci .....	- 26 -
Supplementary Figure 16: 1q42.2-1qter deletions.....	- 27 -
II. Supplementary Tables.....	- 28 -
Supplementary Table 1: Two-sided telomeric repeat loci .....	- 28 -
Supplementary Table 2: siRNA sequences.....	- 28 -
Supplementary Table 3: Antibodies .....	- 28 -
Supplementary Table 4: DEXseq <i>ATRX</i> exon model .....	- 29 -
III. Supplementary References.....	- 30 -

# I. Supplementary Figures



## Supplementary Figure 1: Telomere content and C-Circle intensity of discovery and INFORM cohort

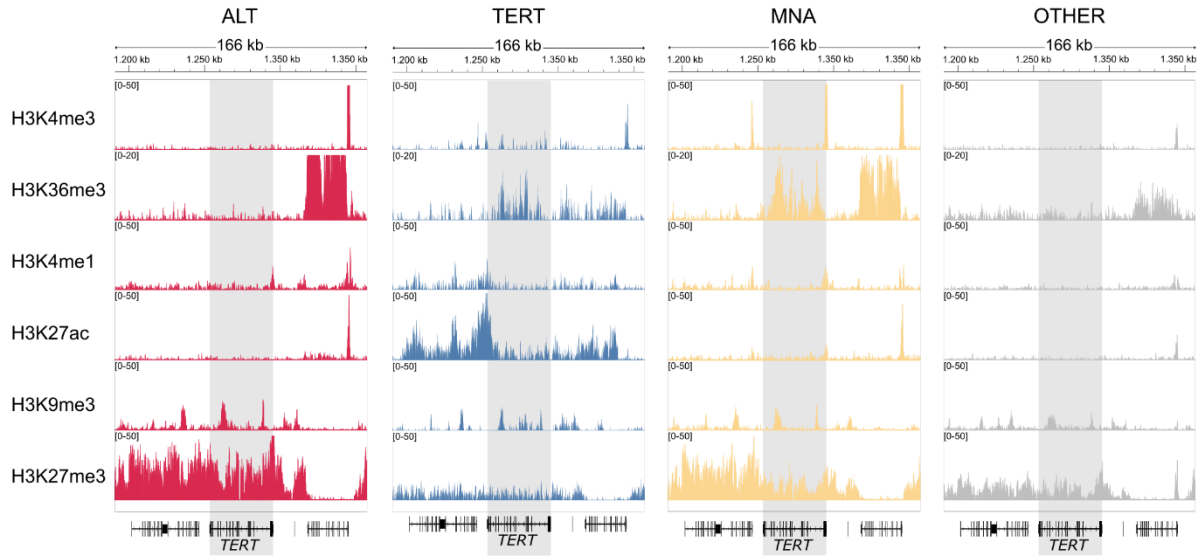
(a) Relative telomere content of C-Circle (CC) positive and negative tumors in the discovery and INFORM cohort. (b) C-Circle intensity relative to CHLA-90 positive control for tumors in the discovery and INFORM cohort. Color-coding indicates the C-Circle status using the two applied criteria of a signal intensity relative to CHLA-90 positive control  $\geq 0.2$  and a signal intensity relative to the negative control without polymerase  $\geq 4$ . Due to the high number of samples, not all tumors could be analyzed on the same blot. Thus, every blot contained a CHLA-90 positive control and signal intensities were normalized to this control. (a-b) Boxplots indicate the median value (middle line) and the 25th and 75th percentiles (box). The upper/lower whisker spans from the hinge to the largest/smallest value (values expanding a distance of 1.5 x inter quartile range are not considered). Dots represent individual tumors.  $P$  values were calculated using two-sided Wilcoxon rank sum tests.  $n$  describes the number of analyzed tumors. (c) Scatter plot of telomere content relative to C-Circle intensity. Color-coding indicates C-Circle status. Correlation coefficient was calculated using spearman correlation.



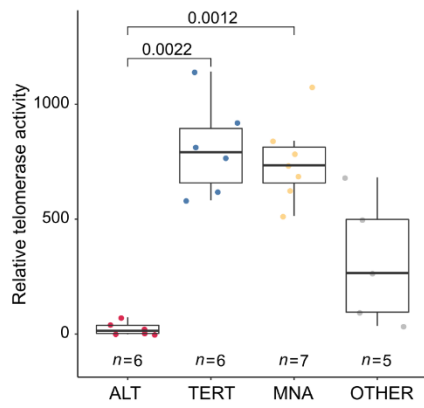
**Supplementary Figure 2: C-Circle status of discovery and INFORM cohort**

C-Circle slot blot images of tumors of the discovery cohort (a) and INFORM cohort (b). Control without polymerase (-Pol) was analyzed for all samples. C-Circle positive tumors are marked in red. Due to the high number of samples, not all tumors could be analyzed on the same blot. Thus, every blot contained a CHLA-90 positive control. Every tumor was analyzed once. Uncut images are shown in source data file.

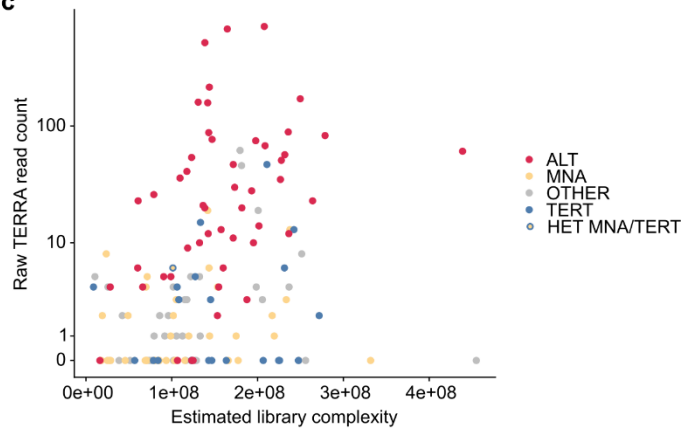
**a**



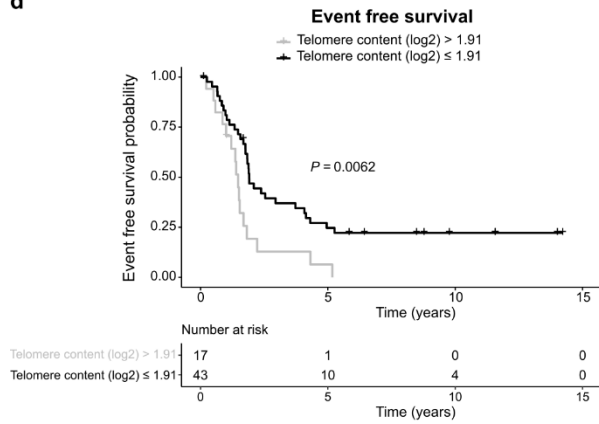
**b**



**c**



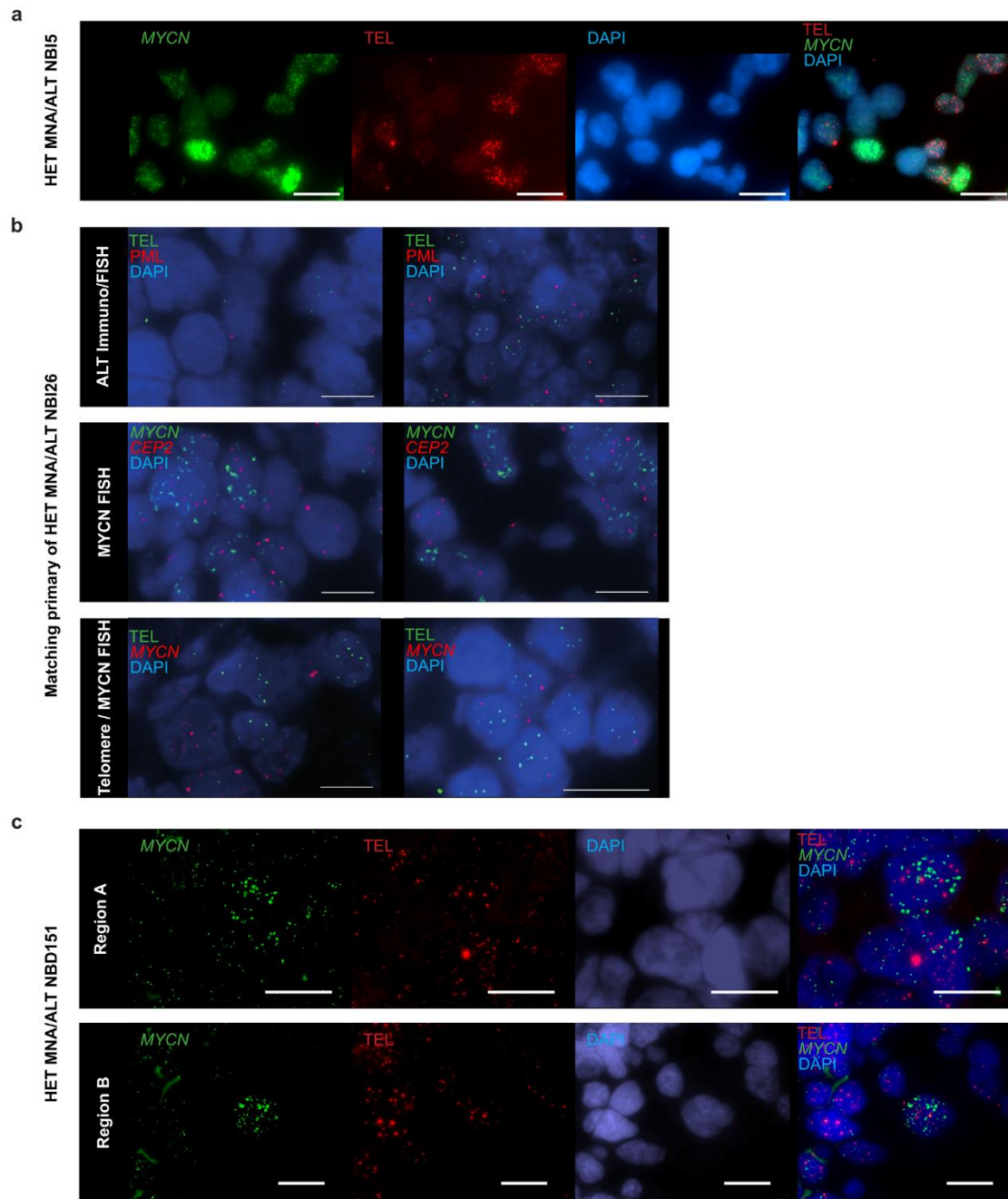
**d**



**Supplementary Figure 3: Silencing of *TERT* locus, telomerase activity and raw TERRA counts**

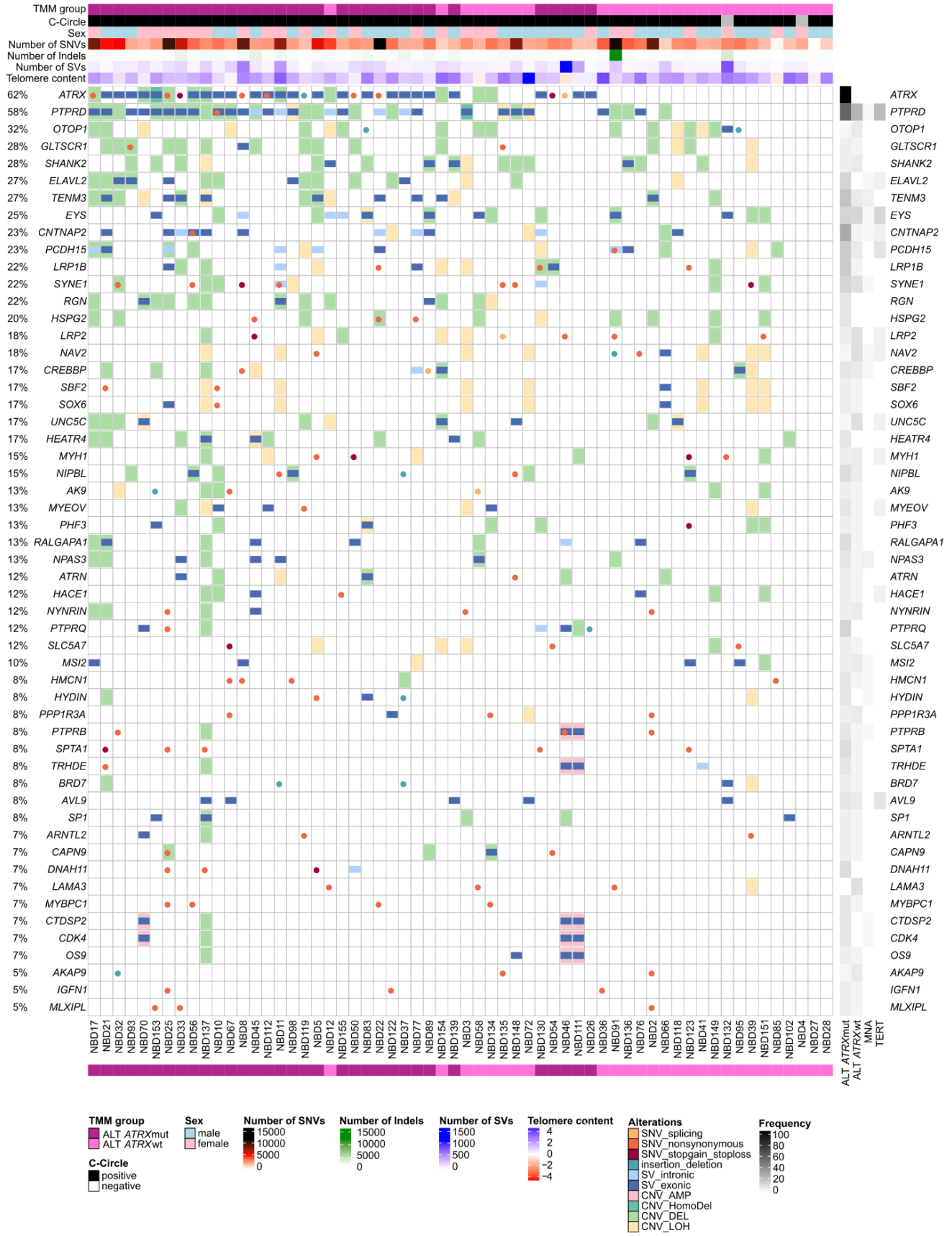
(a) ChIP sequencing profiles of the *TERT* locus of exemplary tumor samples from all subgroups: ALT (red), TERT (blue), MNA (yellow) and OTHER (grey). (b) Relative telomerase activity in different neuroblastoma subgroups: ALT (red), TERT (blue), MNA (yellow) and OTHER (grey). Boxplots indicate the median value (middle line) and the 25th and 75th percentiles (box). The upper/lower whisker spans from the hinge to the largest/smallest value (values expanding a distance of 1.5 x inter quartile range are not considered). Dots represent individual tumors. *n* describes the number of analyzed tumors. *P*-values were calculated using a two-sided Wilcoxon rank sum test. (c) Number of raw TERRA read counts relative to the estimated library complexity. Color-coding indicates TMM group. (d) Event free survival of ALT-positive neuroblastomas in the discovery cohort. ALT-positive tumors are separated based on a very high (>1.91) telomere content. Cut point was calculated using Maximally Selected Rank Statistics. *P* value was calculated using a Log-rank test.





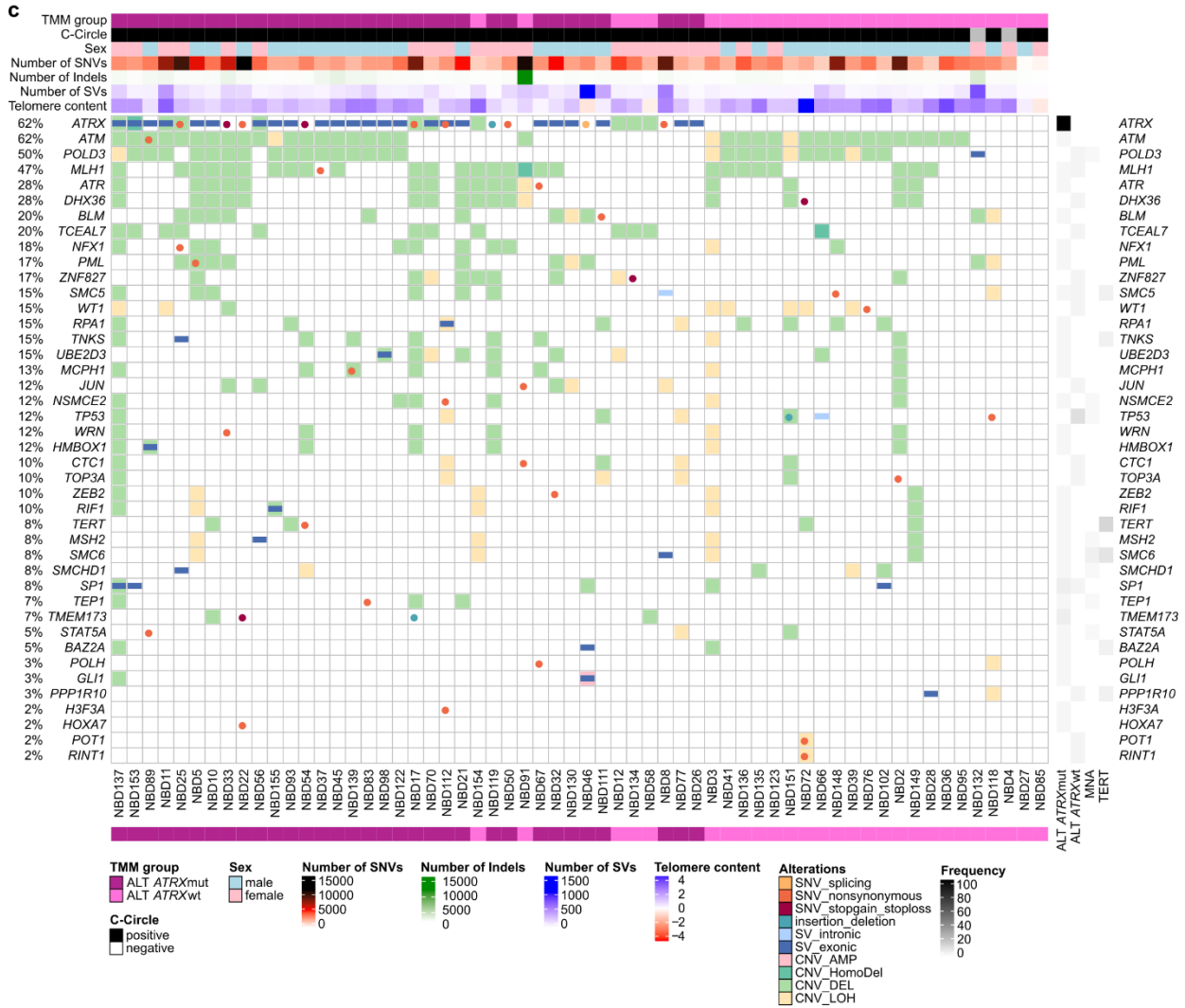
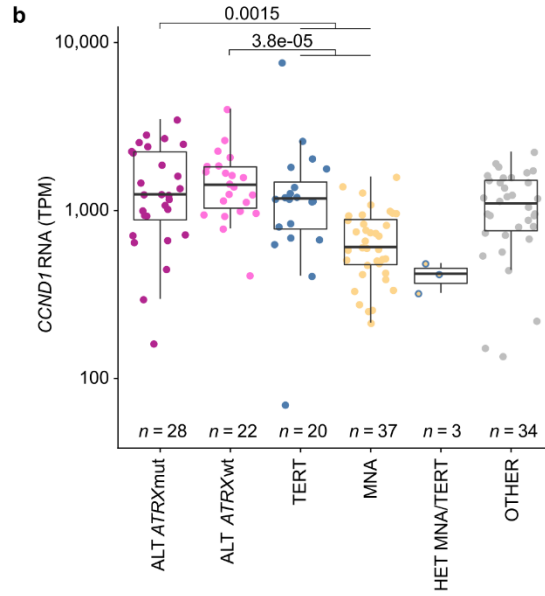
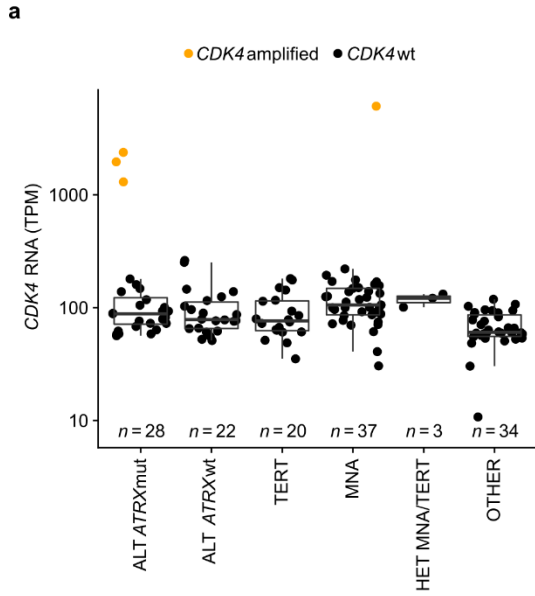
**Supplementary Figure 5: Combined *MYCN* and telomere FISH**

(a) *MYCN* and telomere FISH of HET MNA/ALT tumor NBI5. Additionally, DAPI staining and a merged image are shown. Scale bar representing 20  $\mu$ m. (b) PML immunostaining and telomere FISH of the matching primary of HET MNA/ALT NBI26 (top panel). *MYCN* and *CEP2* FISH of the matching primary of HET MNA/ALT tumor NBI26 (middle panel). *MYCN* and telomere FISH of the matching primary of HET MNA/ALT tumor NBI26 (bottom panel). Scale bar representing 10  $\mu$ m. (c) *MYCN* and telomere FISH of HET MNA/ALT tumor NBD151. Additionally, DAPI staining and a merged image are shown. Scale bar representing 20  $\mu$ m. Every tumor was analyzed once.



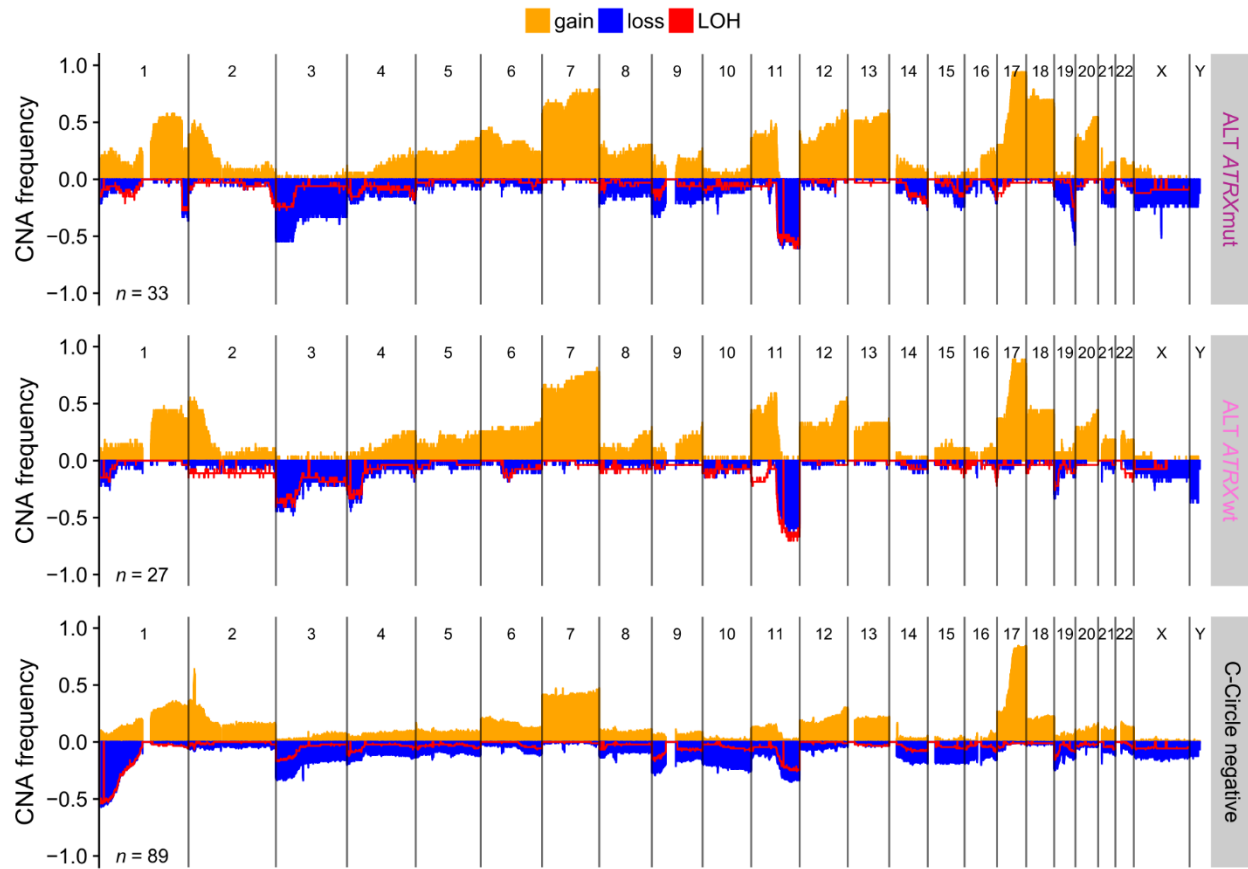
**Supplementary Figure 6: Most frequent differentially mutated genes in ALT-positive tumors**

Somatic alterations were identified in whole genome sequencing data of 60 ALT-positive samples. Exonic single nucleotide variations (SNVs), exonic small insertions and deletions (INDELs), structural variations in exonic and intronic regions (SVs) as well as copy number changes (CNVs) are illustrated. For detailed color-coding and symbols, see legend. See top panel for telomere maintenance features and total number of called SNVs, SVs and INDELs. Frequency calculations on the left are based on SNVs, SVs, INDELs and CNVs. Black and white heatmap on the right side indicates the frequency of mutations of the respective gene in neuroblastoma subgroups. Copy number changes (deletion, LOH) were not considered for frequency calculations in the heatmap (right panel).



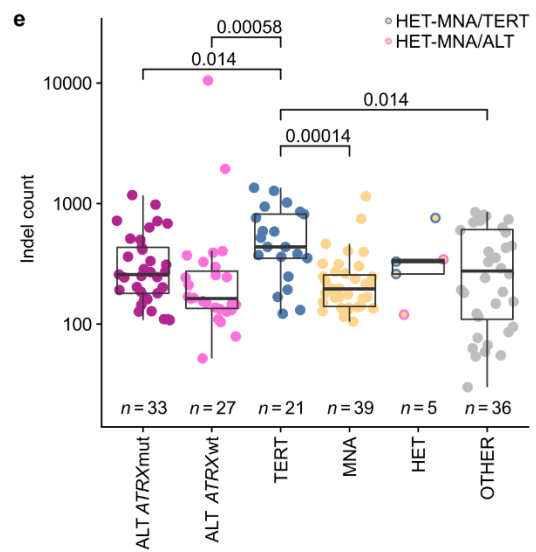
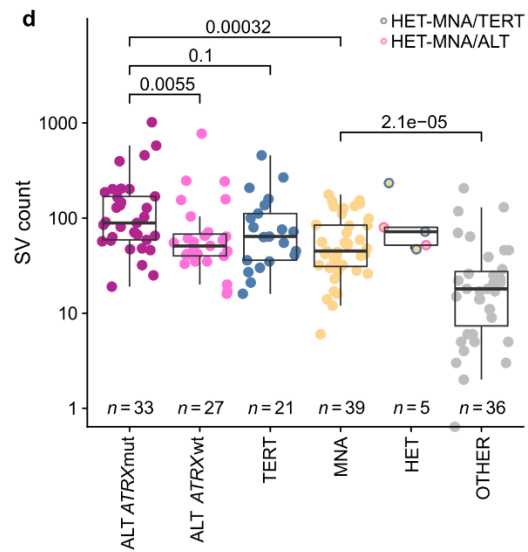
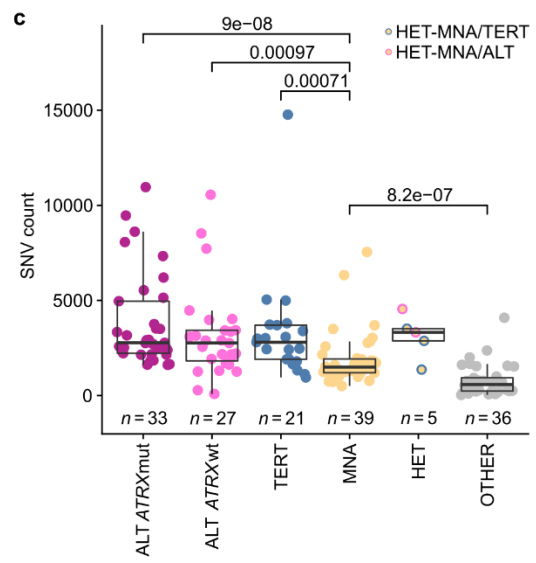
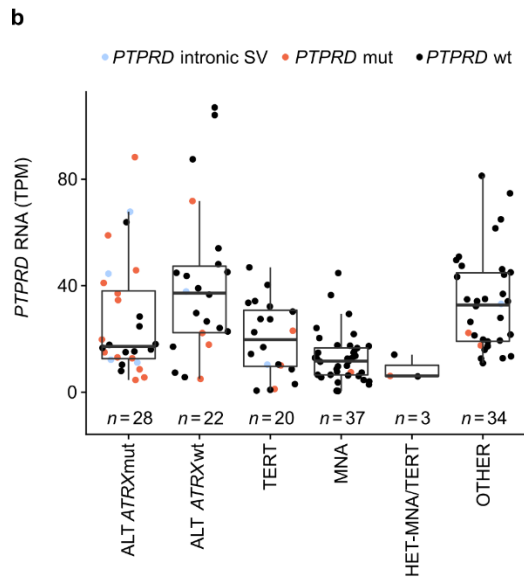
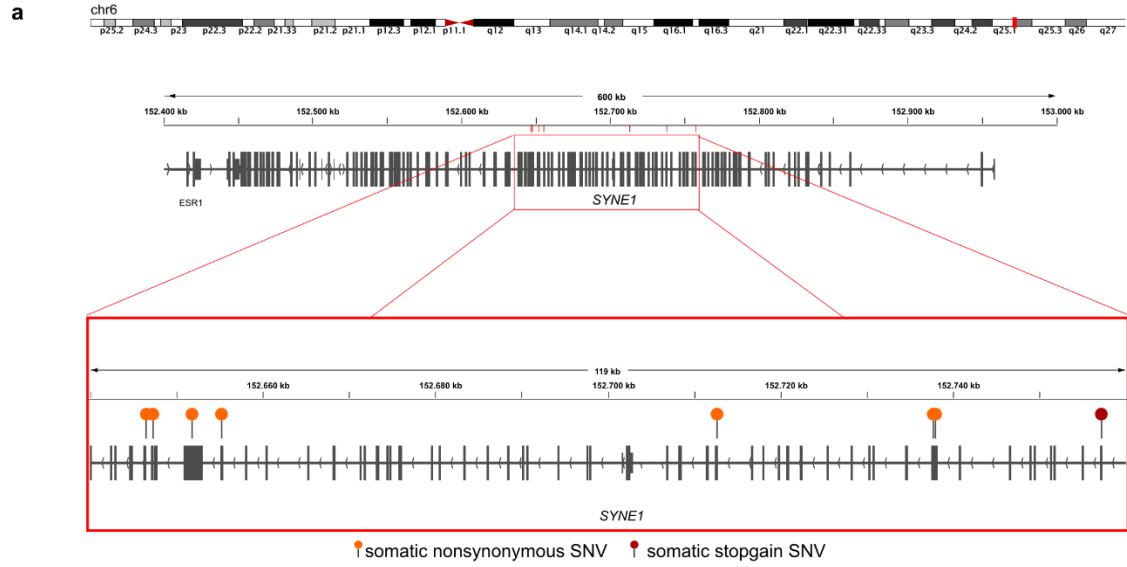
### Supplementary Figure 7: *CDK4/CCND1* expression and mutations in Telnet genes

(a) mRNA expression of *CDK4* in neuroblastoma subgroups. *CDK4* amplified tumors are highlighted. (b) mRNA expression of *CCND1* in neuroblastoma subgroups: ALT *ATRX*-mutated (dark pink), ALT *ATRX* wild-type (light pink), TERT (blue), MNA (yellow) and OTHER (grey) (a-b) Boxplots indicate the median value (middle line) and the 25th and 75th percentiles (box). The upper/lower whisker spans from the hinge to the largest/smallest value (values expanding a distance of 1.5 x inter quartile range are not considered). Dots represent individual tumors. *P* values were calculated with two-sided Wilcoxon rank sum tests. *n* describes the number of analyzed tumors. (c) Mutations in telomere maintenance associated genes in ALT-positive tumors. Somatic alterations were identified in whole genome sequencing data of 60 ALT-positive samples. Only genes reported in the TelNet database as validated to be involved in telomere maintenance<sup>1</sup> are shown. Exonic single nucleotide variations (SNVs), exonic small insertions and deletions (INDELs), structural variations in exonic and intronic regions (SVs) as well as copy number changes are illustrated. See top panel for telomere features and total number of called SNVs, SVs and INDELs. Frequency calculations on the left are based on SNVs, SVs, INDELs and CNVs. Black and white heatmap on the right side indicates the frequency of mutations in the respective gene in neuroblastoma groups of different telomere maintenance mechanisms. Copy number changes (deletion, LOH) were not considered for frequency calculations in the heatmap (right panel).



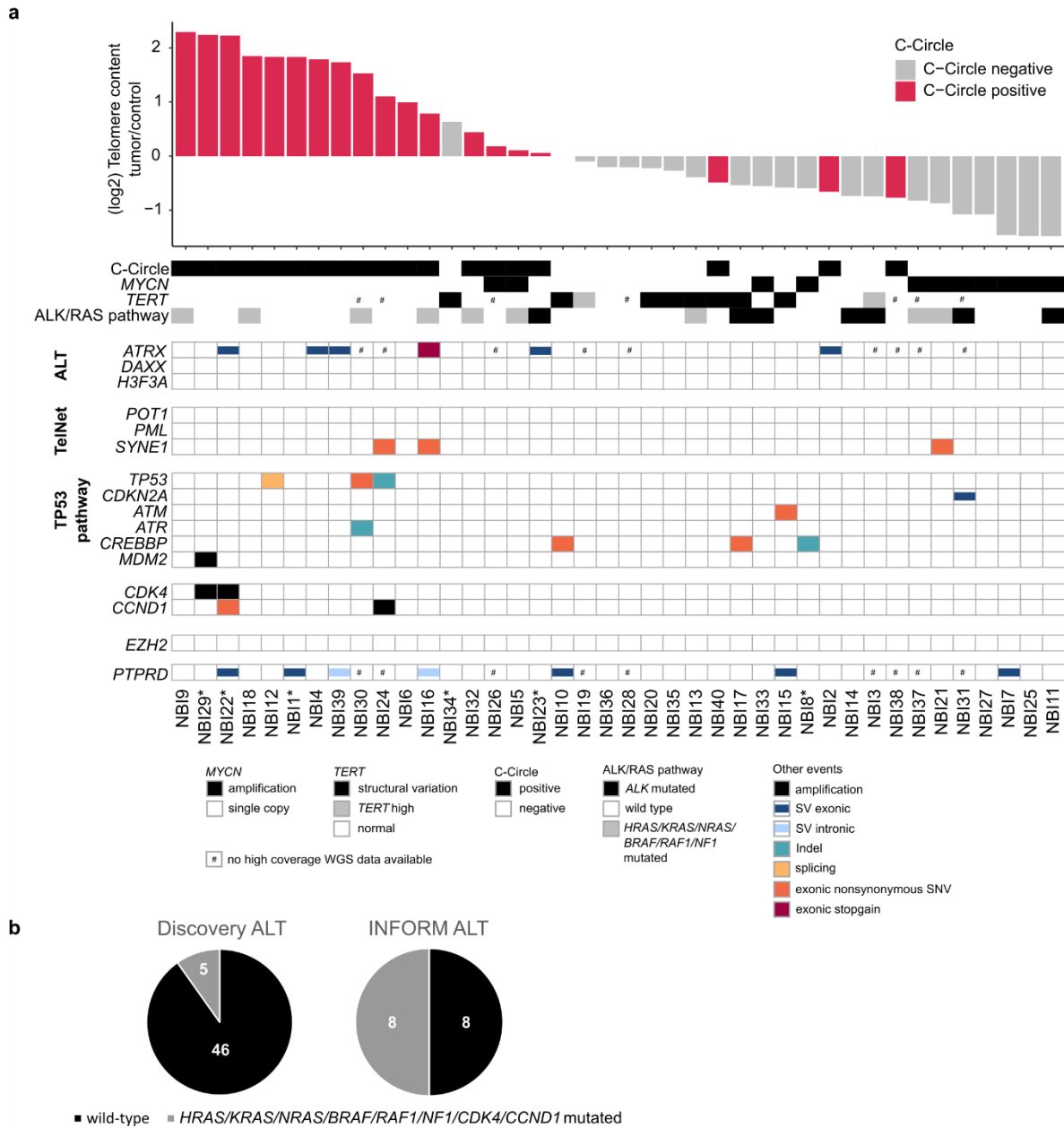
**Supplementary Figure 8: Overall copy number patterns of ALT-positive tumors compared to ALT negative tumors of the discovery cohort.**

CNV frequencies of ALT-positive tumors are further subdivided in *ATRX*-mutated and wild-type. Chromosomes are illustrated along the horizontal axis and frequencies of CNVs along the vertical axis. Gains are illustrated in yellow and losses in blue. LOH is shown as a red line. *n* represents the number of tumors in each group.



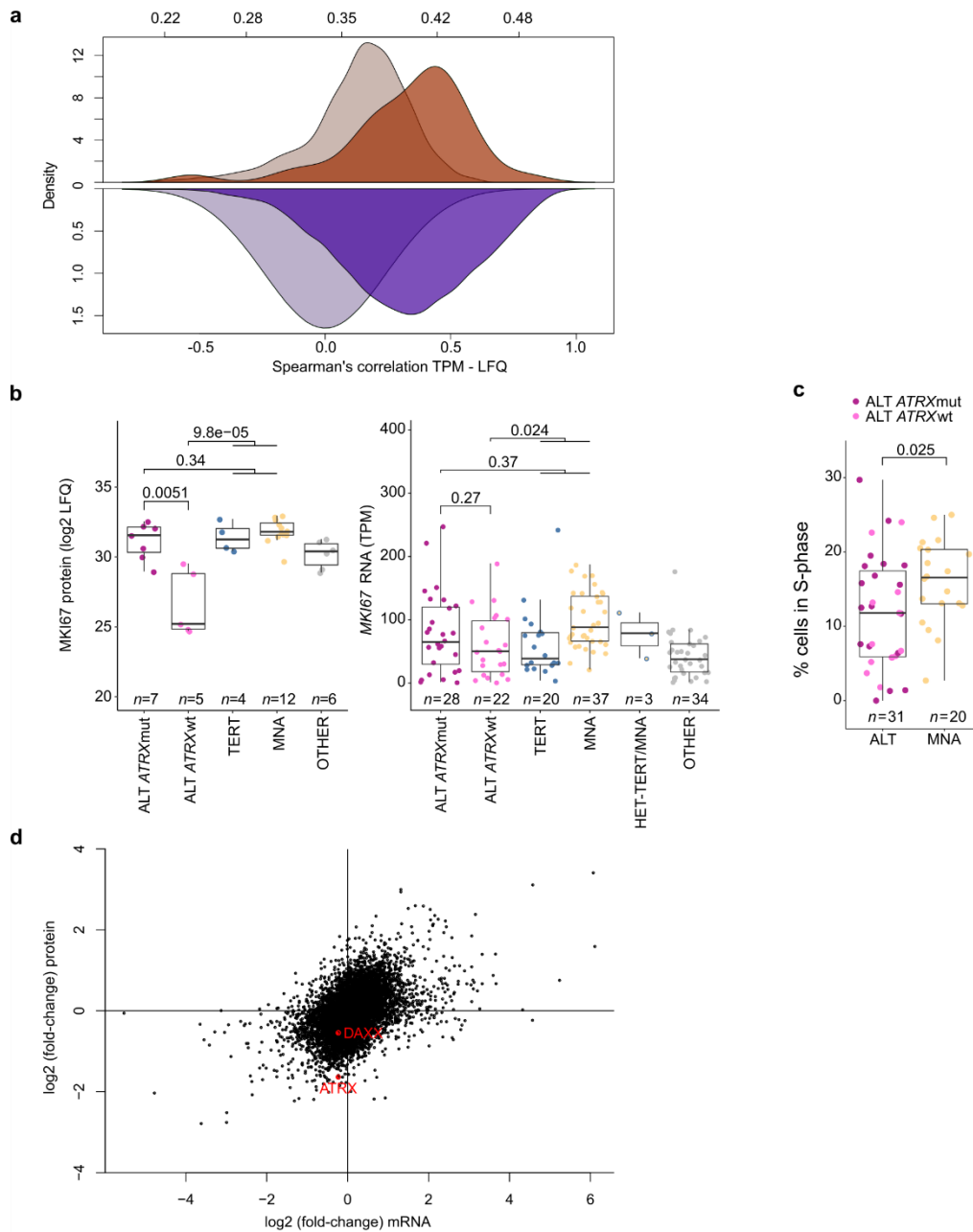
**Supplementary Figure 9: *SYNE1* and *PTPRD***

(a) Exact genomic location of *SYNE1* SNVs. (b) mRNA expression of *PTPRD* in neuroblastoma subgroups. Tumors with *PTPRD* mutations are highlighted. Total number of SNVs (c), SVs (d) and INDELs (e) in the discovery cohort. Samples without a matching blood control sample were excluded from this analysis. (b-e) *P* values were calculated with two-sided Wilcoxon rank sum tests. Boxplots indicate the median value (middle line) and the 25th and 75th percentiles (box). The upper/lower whisker spans from the hinge to the largest/smallest value (values expanding a distance of 1.5 x inter quartile range are not considered). Dots represent individual tumors. *n* describes the number of analyzed tumors. Colors indicate TMM group: ALT *ATRX*-mutated (dark pink), ALT *ATRX* wild-type (light pink), TERT (blue), MNA (yellow) and OTHER (grey).



**Supplementary Figure 10: Mutational landscape of INFORM cohort**

(a) Telomere features and co-mutations in a cohort of relapsed neuroblastomas enrolled in the registry trial INFORM. The top panel indicates telomere maintenance mechanism, relative telomere content (tumor/control) and presence of ALK/RAS pathway mutations (*HRAS*, *NRAS*, *KRAS*, *BRAF*, *RAF1*, *NF1* or *ALK*). Co-mutations in ALT-associated genes, genes associated with telomere biology according to the TelNet database<sup>1</sup> and TP53 pathway genes are shown. Somatic co-mutations of relapsed patients were identified using WES and low coverage WGS data. *ATRX* mutations, *TERT* SVs and *PTPRD* SVs were analyzed using high coverage whole genome sequencing (# no high coverage WGS data was available). \*) Sample is part of a matching primary relapse pair. (b) Frequency of RAS pathway mutations (*HRAS*, *KRAS*, *NRAS*, *BRAF*, *RAF1*, *NF1*, *CDK4*, *CCND1*) in ALT-positive neuroblastomas in the discovery and INFORM cohort. Relapse cases in the discovery cohort and HET cases in the INFORM cohort were excluded from the analysis.



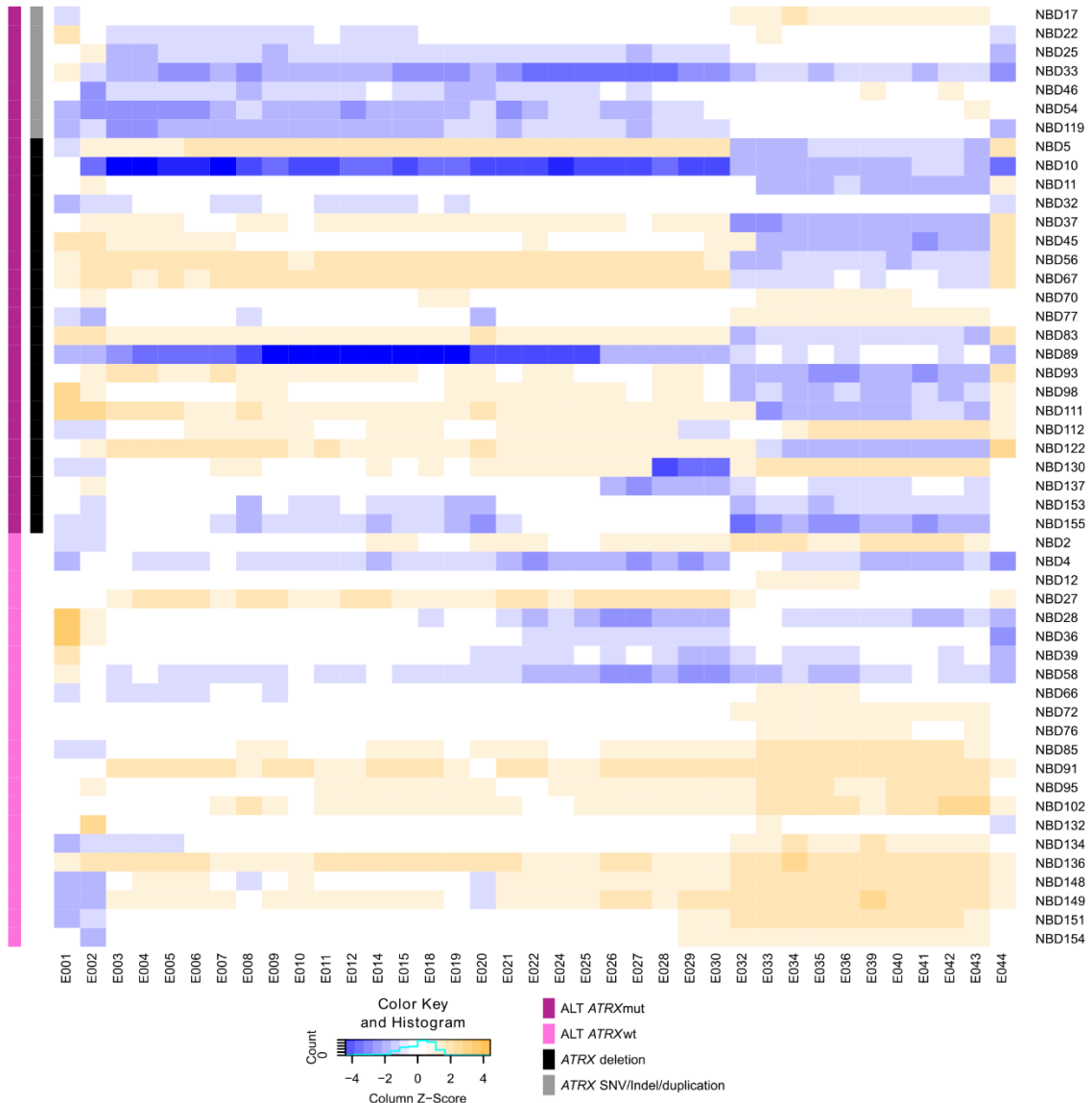
### Supplementary Figure 11: Comparison of mRNA and protein data

(a) Distributions of Spearman's correlation coefficients between mRNA and protein abundance. (top) between different transcript-protein pairs per matching tumor sample (orange, mean Spearman's correlation coefficient = 0.4) and with random tumor sample (grey, mean Spearman's correlation coefficient = 0.36). (bottom) between varying abundances of transcript and proteins per matching genes (with at least 10 paired measurements) (purple, mean Spearman's correlation coefficient = 0.32) and with random gene (grey, mean Spearman's correlation coefficient = 0).

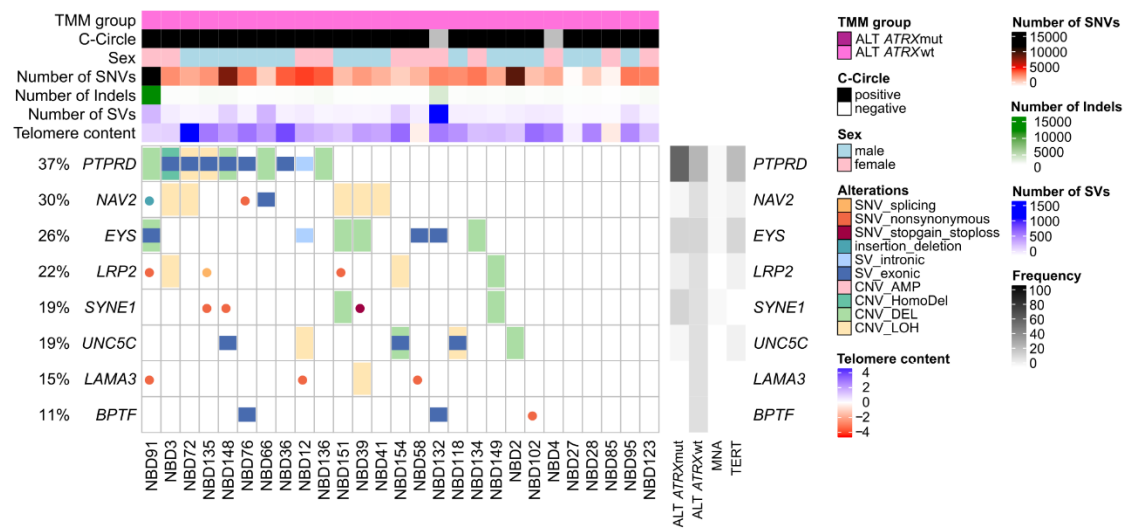
(b) Protein and mRNA expression of *MKI67* in neuroblastoma tumors of the discovery cohort. (c) Percentage of cells in S-phase compared between ALT-positive and MNA tumors determined by FACS analysis of  $n = 51$  cases. (b-c) Colors indicate TMM group: ALT *ATRX*-mutated (dark pink), ALT *ATRX* wild-type (light pink), TERT (blue), MNA (yellow) and OTHER (grey). Boxplots indicate the median value (middle line) and the 25th and 75th

percentiles (box). The upper/lower whisker spans from the hinge to the largest/smallest value (values expanding a distance of 1.5 x inter quartile range are not considered). Dots represent individual tumors. *P* values were calculated with two-sided Wilcoxon rank sum tests. *n* describes the number of analyzed tumors. (d) Comparison of mRNA and protein fold-changes between ALT tumors and neuroblastomas of the other TMM groups (MNA, TERT, OTHER).

**a**

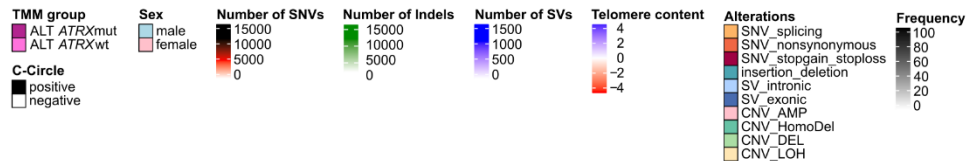
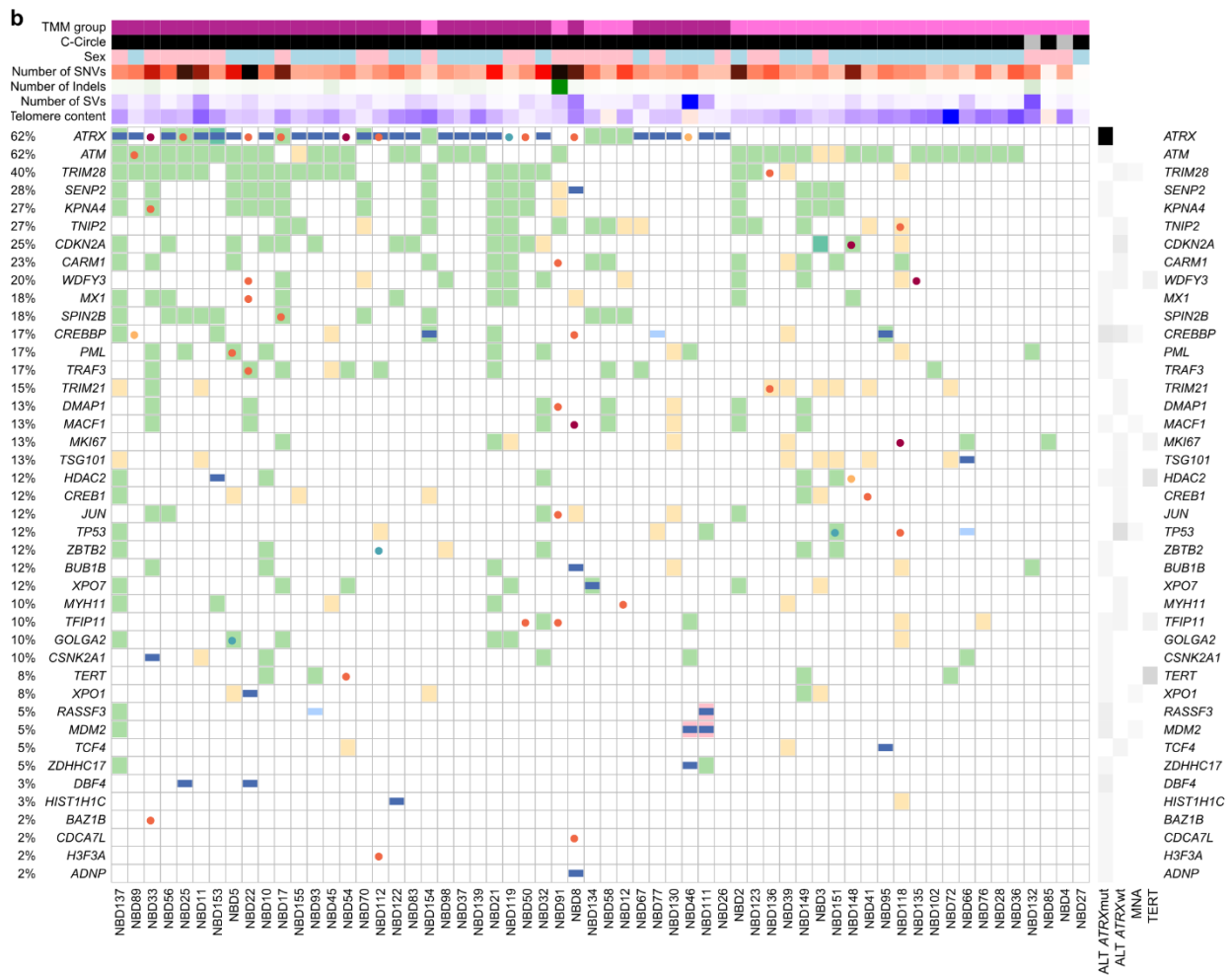
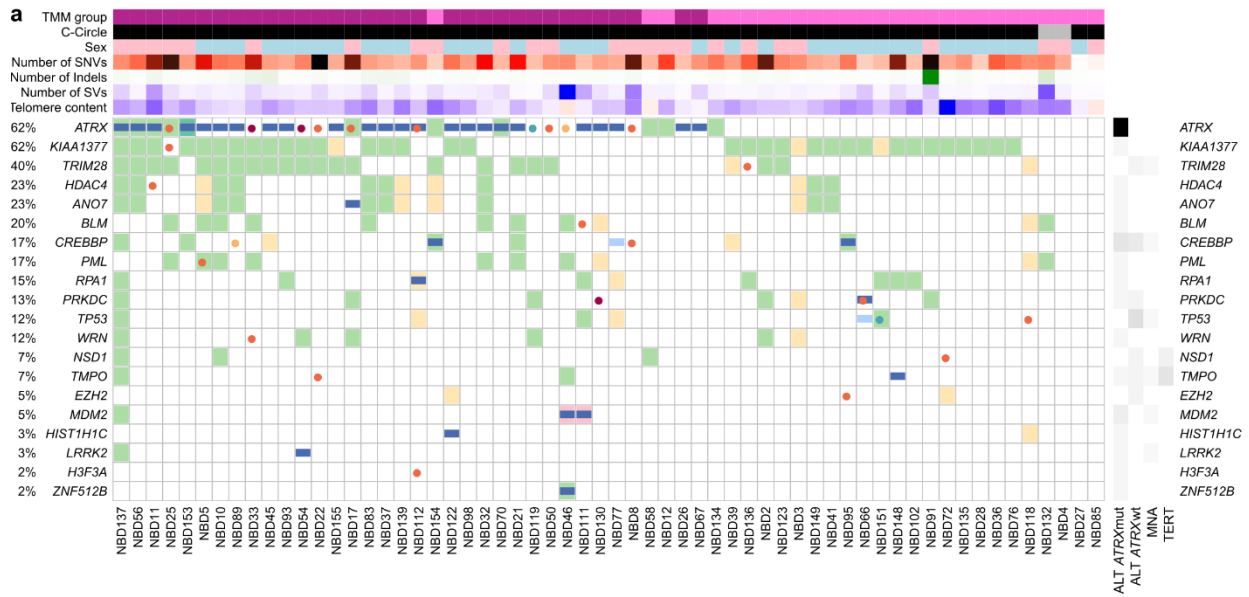


**b**



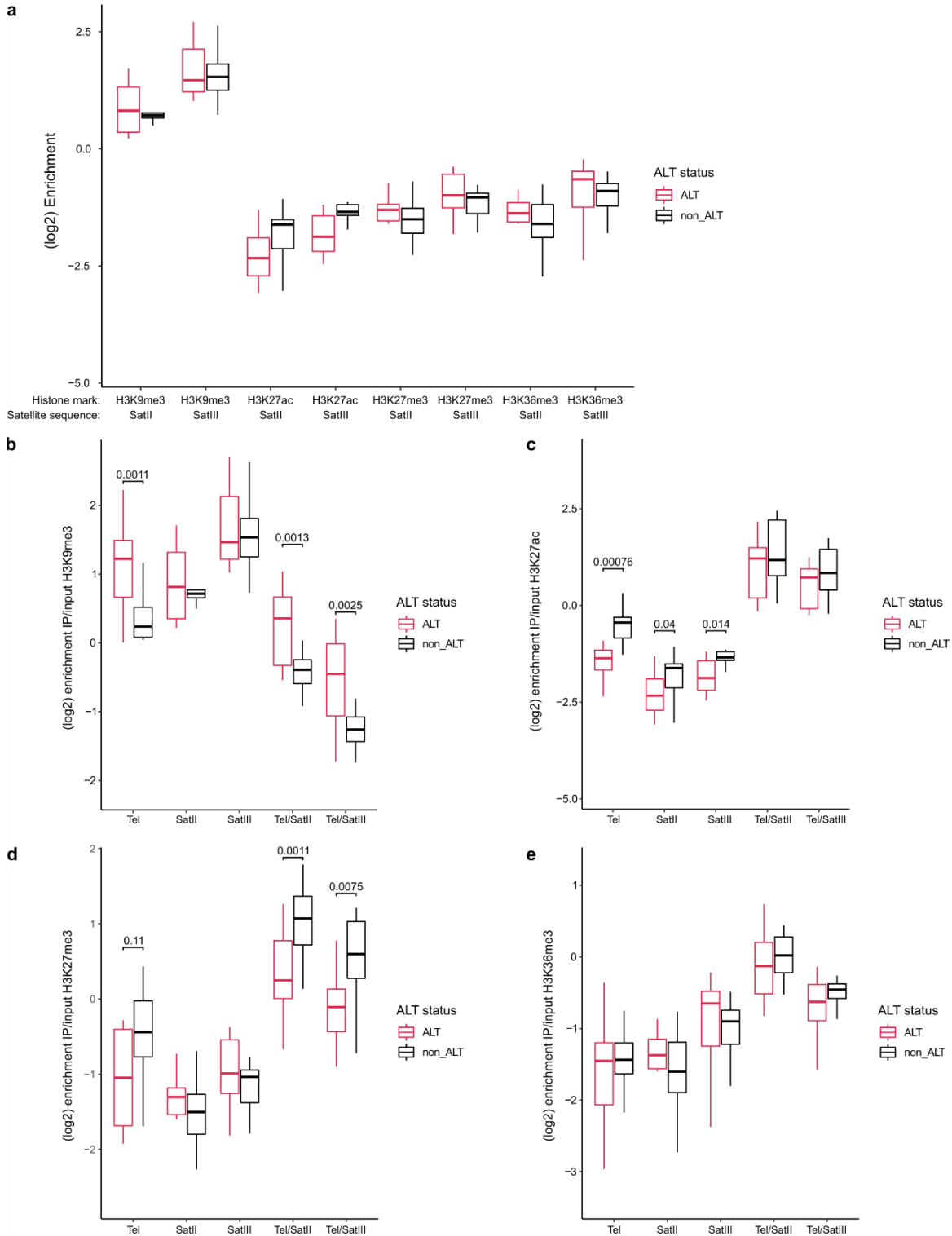
**Supplementary Figure 12: Exon specific expression of *ATRX* and most frequent mutations in ALT-positive *ATRX* wild-type neuroblastomas**

(a) *ATRX* per exon normalized mRNA expression. mRNA expression (log<sub>2</sub> RPKM) per exon (E1-E44) of *ATRX* in ALT neuroblastomas. Tumors with *ATRX* deletions are compared to tumors with other *ATRX* mutations and *ATRX* wild-type tumors. See Supplementary Table 4 for *ATRX* exon model. (b) Most recurrent mutations in ALT-positive *ATRX*wt neuroblastomas. Only genes with at least three exonic events (SVs, INDELs, SNVs) are shown. Exonic single nucleotide variations (SNVs), exonic small insertions and deletions (INDELs), structural variations in exonic and intronic regions (SVs) as well as copy number changes are illustrated. See top panel for telomere features and total number of called SNVs, SVs and INDELs. Frequency calculations on the left are based on SNVs, SVs, INDELs and CNVs. Black and white heatmap on the right side indicates the frequency of mutations in the respective gene in neuroblastoma groups of different telomere maintenance mechanisms. Copy number changes (deletion, LOH) were not considered for frequency calculations in the heatmap (right panel).



**Supplementary Figure 13: Mutations in ATRX/DAXX interaction partners**

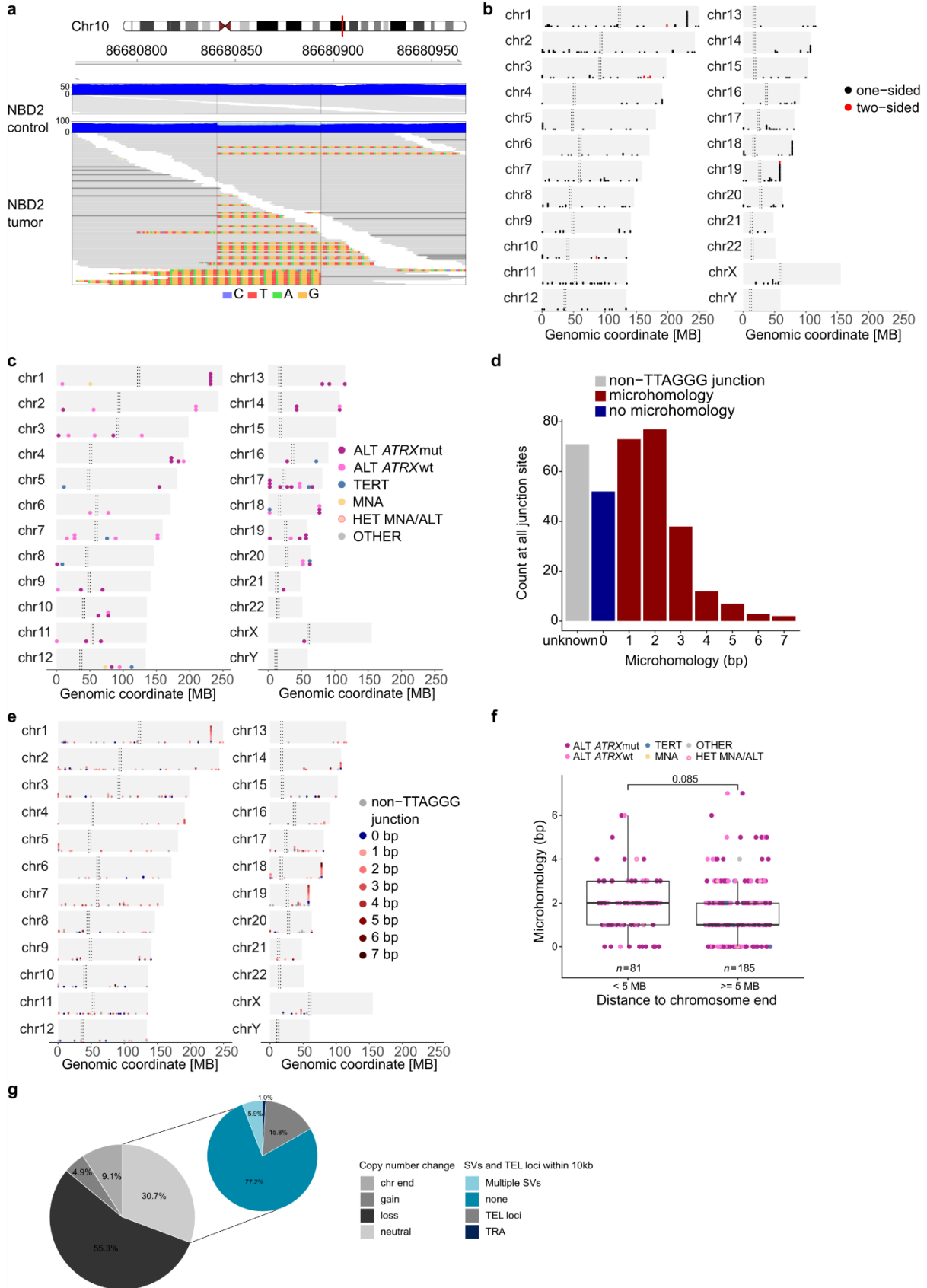
Mutations of ATRX (a) and DAXX (b) interaction partners in ALT-positive neuroblastomas. ATRX and DAXX interaction partners were obtained from BioGRID [<https://thebiogrid.org/>]. Only genes with at least one exonic event (SVs, INDELs, SNVs) are shown. Exonic single nucleotide variations (SNVs), exonic small insertions and deletions (INDELs), structural variations in exonic and intronic regions (SVs) as well as copy number changes are illustrated. See top panel for telomere features and total number of called SNVs, SVs and INDELs. Frequency calculations on the left are based on SNVs, SVs, INDELs and CNVs. Black and white heatmap on the right side indicates the frequency of mutations in the respective gene in neuroblastoma groups of different telomere maintenance mechanisms. Copy number changes (deletion, LOH) were not considered for frequency calculations in the heatmap (right panel).



**Supplementary Figure 14: Chromatin state at SatII and SatIII sequences**

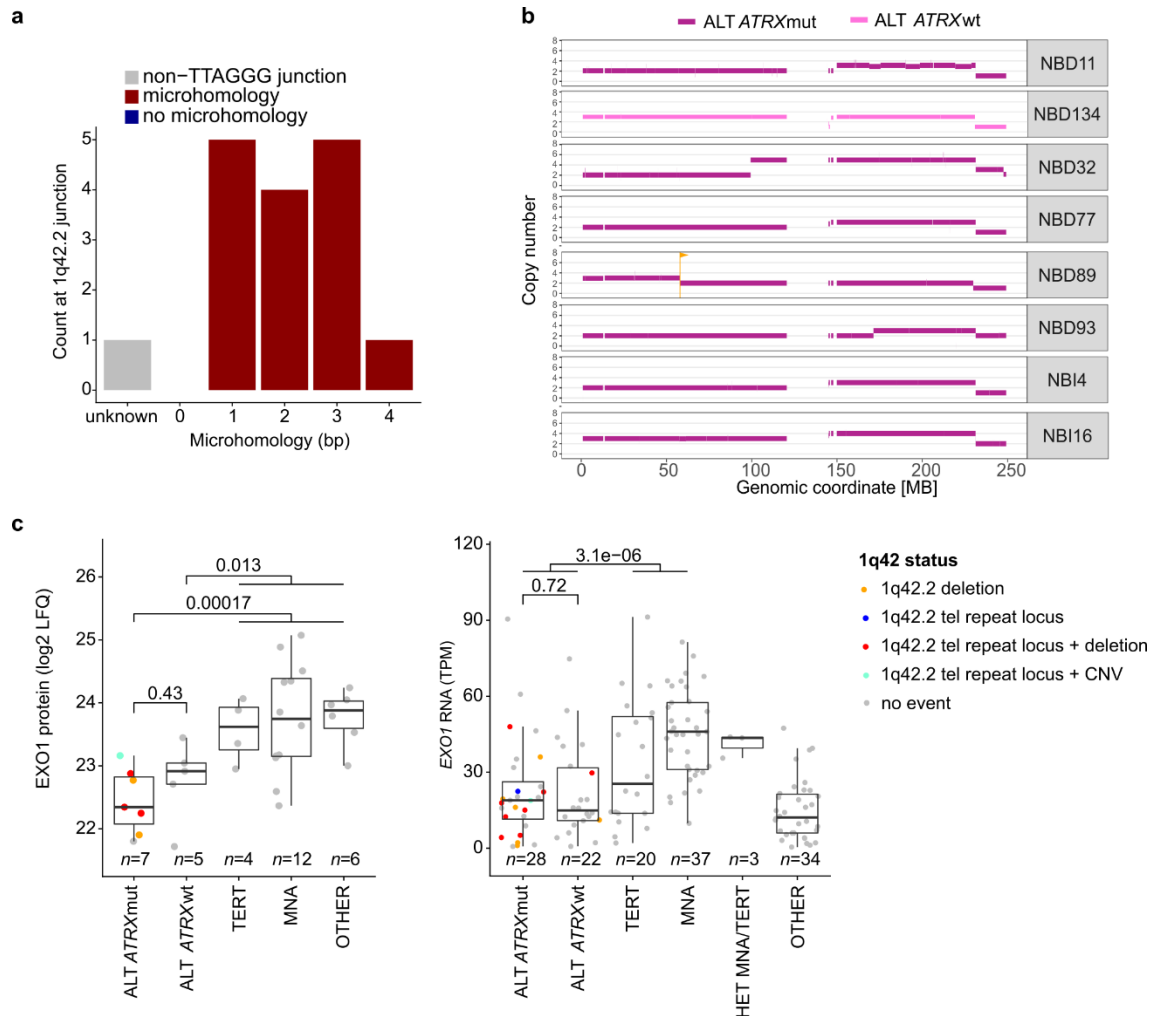
(a) log<sub>2</sub> enrichment of ChIP signals relative to input signals of SatII and SatIII sequences for H3K9me<sub>3</sub>, H3K27ac, H3K27me<sub>3</sub> and H3K36me<sub>3</sub>. ALT-positive tumors were compared to ALT-negative tumors (b-e) log<sub>2</sub> enrichment in ChIP of H3K9me<sub>3</sub> (b, *n* = 26), H3K27ac (c, *n* = 25), H3K27me<sub>3</sub> (d, *n* = 25) and

H3K36me3 (e,  $n = 27$ ) relative to input. Enrichment at telomeres, SatII and SatIII sequences is given. Additionally, telomeric signals were normalized to either SatII or SatIII. ALT-positive tumors are compared to ALT-negative tumors. Boxplots indicate the median value (middle line) and the 25th and 75th percentiles (box). The upper/lower whisker spans from the hinge to the largest/smallest value (values expanding a distance of 1.5 x inter quartile range are not considered).  $n$  describes the number of analyzed tumors.  $P$ -values were calculated using two-sided Wilcoxon rank sum tests.



### Supplementary Figure 15: Features of telomeric repeat loci

(a) Example of two telomeric repeat loci forming a two-sided or insertion-like event. Dark blue color indicates sequencing coverage and light blue color illustrates clipped sequences. Reads are shown in medium grey and clipped bases are color-coded. Non-telomeric ends of a discordant read pair are labeled in dark grey. (b) Chromosomal location of one-sided and two-sided telomeric repeat loci of the discovery cohort. (c) Chromosomal location of telomeric repeat loci in the INFORM cohort. (d) The occurrence of homologous bases (microhomology) between the reference genome and TTAGGG telomere repeats was counted for all telomeric repeat loci in the discovery cohort. (e) Degree of microhomology (color-coding) and chromosomal location for all telomeric repeat loci in the discovery cohort. (f) Degree of microhomology to TTAGGG of telomeric repeat loci being less than 5 MB or more than 5 MB away from the chromosome end. Boxplots indicate the median value (middle line) and the 25th and 75th percentiles (box). The upper/lower whisker spans from the hinge to the largest/smallest value (values expanding a distance of 1.5 x inter quartile range are not considered). Dots represent individual telomeric repeat loci. *n* gives the number of telomeric repeat loci in each group. *P*-value was calculated using a two-sided Wilcoxon rank sum test. (g) (left pie) Percentage of telomeric repeat loci overlapping with a copy number variation (events in group “chr end” are too close to the telomere and thus no CNV information could be obtained). (right pie) Percentage of copy number neutral telomeric repeat loci overlapping with an SV breakpoint within a 10 kb window (TRA = translocation, TEL loci = another telomeric repeat locus, Multiple SVs = more than one SV in 10 kb distance, none = no SV in 10kb window).



### Supplementary Figure 16: 1q42.2-1qter deletion

(a) The occurrence of homologous bases between the reference genome and TTAGGG telomere repeats was counted for all telomeric repeat loci at the 1q42.2 hotspot. 1q42.2 telomeric repeat loci of NBD25 were excluded as they had a different directionality. (b) Chr1 copy number profile of tumors with a 1q42.2-1qter deletion without a detected telomeric repeat locus color coded by subgroup. chr1q42.2-1qter deletion was defined as a reduced copy number compared to the upstream neighboring segment. (c) Boxplots of protein and mRNA expression of *EXO1* in ALT *ATRX*-mutated and wild-type tumors compared to TERT, MNA and tumors without a telomere maintenance mechanism (OTHER). Colors indicate the presence of a telomeric repeat locus on chr1q42.2 and/or presence of a chr1q42.2-1qter deletion (compared to the neighboring upstream segment). Boxplots indicate the median value (middle line) and the 25th and 75th percentiles (box). The upper/lower whisker spans from the hinge to the largest/smallest value (values expanding a distance of 1.5 x inter quartile range are not considered). Dots represent individual tumors. *n* describes the number of analyzed tumors. *P* values were calculated with two-sided Wilcoxon rank sum tests.

## II. Supplementary Tables

**Supplementary Table 1: Two-sided telomeric repeat loci**

ID	Chr	Junction 1 <sup>a</sup>	Junction 2 <sup>a</sup>	Distance <sup>b</sup>	Supporting read pairs <sup>c</sup>
NBD11	3	171927766	171927838	72	0
NBD22	19	57621777	57622140	363	0
NBD5	3	162504712	162506720	2008	10
NBD130	1	198923306	198923309	3	2
NBD2	10	86680841	86680894	53	0

<sup>a</sup> Chromosomal position of junction sites of contributing telomeric repeat loci

<sup>b</sup> Distance between the two junction sites

<sup>c</sup> Number of read pairs supporting an insertion like event, meaning that mates of a read pair map to both sides of the event

**Supplementary Table 2: siRNA sequences**

siRNAs	Sequence/ siRNA ID	Supplier
ATRX si1 (sh589) <sup>a</sup>	5'-GCAGATTGATATGAGAGGAAT-3'	Ambion Silencer™ select siRNA (custom)
ATRX si2 (sh590) <sup>a</sup>	5'-CGACAGAACTAACCCCTGTAA-3'	Ambion Silencer™ select siRNA (custom)
ATRX si3 (sh592) <sup>a</sup>	5'-CCGGTGGTGAACATAAGAAAT-3'	Ambion Silencer™ select siRNA (custom)
DAXX si1	s3935	Ambion Silencer™ select siRNA
DAXX si2	s3936	Ambion Silencer™ select siRNA
DAXX si3	s3937	Ambion Silencer™ select siRNA
Negative Control No. 1	4390843	Ambion Silencer™ select siRNA
Negative Control No. 2	4390846	Ambion Silencer™ select siRNA

<sup>a</sup> ATRX siRNA target sequences were taken from<sup>2</sup> and obtained from Thermo Fisher as custom silencer select siRNA

**Supplementary Table 3: Antibodies**

Target	Species	Clone	Supplier	Dilution	Order No.	Lot. No.
ATRX	rabbit	polyclonal	Sigma	1:1000	HPA001906	CI118688
DAXX	rabbit	monoclonal E94	Abcam	1:5000	ab32140	GR155454-9
Vinculin-HRP	mouse	monoclonal 7F9	Santa Cruz	1:1000	sc73614	A2319
Secondary rabbit-HRP	goat	polyclonal	Dianova	1:2000	111-035-144	134896
H3K27me3	rabbit	polyclonal	Active Motif	3µg/IP	39155	31014017
H3K36me3	rabbit I	polyclonal	Abcam	3µg/IP	ab9050	GR273250-1
H3K9me3	rabbit	polyclonal	Abcam	3µg/IP	ab8898	GR148830-2
H3K27ac	rabbit	polyclonal	Abcam	3µg/IP	ab4729	GR183919-2
anti-dig-FITC antibody	sheep	polyclonal	Roche	1:100	11207741910	11404500

**Supplementary Table 4: DEXseq *ATRX* exon model**

Exon	ID	Chr	Start	End	Width	Strand
ENSG00000085224.16:E001	E001	chrX	76760356	76760377	22	-
ENSG00000085224.16:E002	E002	chrX	76760378	76764107	3730	-
ENSG00000085224.16:E003	E003	chrX	76776266	76776394	129	-
ENSG00000085224.16:E004	E004	chrX	76776881	76776976	96	-
ENSG00000085224.16:E005	E005	chrX	76777741	76777866	126	-
ENSG00000085224.16:E006	E006	chrX	76778730	76778879	150	-
ENSG00000085224.16:E007	E007	chrX	76812922	76813116	195	-
ENSG00000085224.16:E008	E008	chrX	76814140	76814317	178	-
ENSG00000085224.16:E009	E009	chrX	76829715	76829823	109	-
ENSG00000085224.16:E010	E010	chrX	76845304	76845410	107	-
ENSG00000085224.16:E011	E011	chrX	76849166	76849319	154	-
ENSG00000085224.16:E012	E012	chrX	76854880	76855049	170	-
ENSG00000085224.16:E013	E013	chrX	76855201	76855203	3	-
ENSG00000085224.16:E014	E014	chrX	76855204	76855289	86	-
ENSG00000085224.16:E015	E015	chrX	76855903	76856033	131	-
ENSG00000085224.16:E016	E016	chrX	76856034	76856224	191	-
ENSG00000085224.16:E017	E017	chrX	76871720	76871979	260	-
ENSG00000085224.16:E018	E018	chrX	76872081	76872198	118	-
ENSG00000085224.16:E019	E019	chrX	76874274	76874449	176	-
ENSG00000085224.16:E020	E020	chrX	76875863	76876000	138	-
ENSG00000085224.16:E021	E021	chrX	76888695	76888872	178	-
ENSG00000085224.16:E022	E022	chrX	76889054	76889200	147	-
ENSG00000085224.16:E023	E023	chrX	76889913	76890084	172	-
ENSG00000085224.16:E024	E024	chrX	76890085	76890194	110	-
ENSG00000085224.16:E025	E025	chrX	76891406	76891547	142	-
ENSG00000085224.16:E026	E026	chrX	76907604	76907843	240	-
ENSG00000085224.16:E027	E027	chrX	76909588	76909690	103	-
ENSG00000085224.16:E028	E028	chrX	76912050	76912143	94	-
ENSG00000085224.16:E029	E029	chrX	76918871	76919047	177	-
ENSG00000085224.16:E030	E030	chrX	76920134	76920267	134	-
ENSG00000085224.16:E031	E031	chrX	76931535	76931720	186	-
ENSG00000085224.16:E032	E032	chrX	76931721	76931793	73	-
ENSG00000085224.16:E033	E033	chrX	76937012	76937093	82	-
ENSG00000085224.16:E034	E034	chrX	76937094	76940085	2992	-
ENSG00000085224.16:E035	E035	chrX	76940431	76940498	68	-
<i>ENSG00000085224.16:E036</i>	E036	chrX	76944311	76944420	110	-
ENSG00000085224.16:E037	E037	chrX	76946296	76946418	123	-
ENSG00000085224.16:E038	E038	chrX	76949188	76949312	125	-
ENSG00000085224.16:E039	E039	chrX	76949313	76949426	114	-
ENSG00000085224.16:E040	E040	chrX	76952065	76952192	128	-
ENSG00000085224.16:E041	E041	chrX	76953071	76953123	53	-
ENSG00000085224.16:E042	E042	chrX	76954062	76954117	56	-
ENSG00000085224.16:E043	E043	chrX	76972608	76972720	113	-
ENSG00000085224.16:E044	E044	chrX	77041468	77041702	235	-

### III. Supplementary References

- 1 Braun, D. M., Chung, I., Kepper, N., Deeg, K. I. & Rippe, K. TelNet - a database for human and yeast genes involved in telomere maintenance. *BMC Genet* **19**, 32, doi:10.1186/s12863-018-0617-8 (2018).
- 2 Lovejoy, C. A. *et al.* Loss of ATRX, genome instability, and an altered DNA damage response are hallmarks of the alternative lengthening of telomeres pathway. *PLoS Genet* **8**, e1002772, doi:10.1371/journal.pgen.1002772 (2012).